

Spontaneous symmetry breaking in a polariton and photon laser

H. Ohadi,¹ E. Kammann,¹ T.C.H. Liew,² K.G. Lagoudakis,³ A.V. Kavokin,^{4,1} and P.G. Lagoudakis^{1,*}

¹*School of Physics and Astronomy, University of Southampton, Southampton, SO17 1BJ, United Kingdom*

²*Mediterranean Institute of Fundamental Physics, 31, via Appia Nuova, 00040, Rome, Italy*

³*Stanford University, 348 Via Pueblo Mall, Stanford, CA 94305-4088, US*

⁴*Spin Optics Laboratory, St. Petersburg State University,
1, Uljanovskaya, St. Petersburg, 198504, Russia*

(Dated: March 3, 2013)

We report on the simultaneous observation of spontaneous symmetry breaking and long-range spatial coherence both in the strong and the weak-coupling regime in a semiconductor microcavity. Under pulsed excitation, the formation of a stochastic order parameter is observed in polariton and photon lasing regimes. Single-shot measurements of the Stokes vector of the emission exhibit the buildup of stochastic polarization. Below threshold, the polarization noise does not exceed 10%, while above threshold we observe a total polarization of up to 50% after each excitation pulse, while the polarization averaged over the ensemble of pulses remains nearly zero. In both polariton and photon lasing regimes, the stochastic polarization buildup is accompanied by the buildup of spatial coherence. We find that the Landau criterion of spontaneous symmetry breaking and Penrose-Onsager criterion of long-range order for Bose-Einstein condensation are met in both polariton and photon lasing regimes.

Bosonic particles cooled below the temperature of quantum degeneracy undergo a thermodynamic phase transition during which phase correlations spontaneously build up and the system enters a macroscopic coherent state. This process is known as Bose-Einstein condensation (BEC). BEC is characterised by a buildup of an order parameter, which is usually associated with a macroscopic multi-particle wave function of the condensate [1]. Recently, observation of BEC of exciton-polaritons in CdTe, GaAs and GaN-based microcavities has been claimed by several groups [2–5]. Several features of BEC have indeed been observed, such as: the macroscopic occupation of a quantum state on top of a Boltzmann-like distribution, the long-range spatial coherence, the spectral narrowing of the photoluminescence signal and the decrease of the second order coherence. While necessary, these signatures are not unambiguous proofs of BEC in exciton-polariton planar microcavities simply due to the fact that these features have also been reported in conventional lasers [vertical cavity surface emitting lasers (VCSELs)] [6, 7]. The terminology used in describing degenerate polariton gases is still a subject of debate in the scientific community ranging from polariton BEC to polariton laser [8, 9]. More recently BEC of photons was reported in a weakly-coupled dye-filled microcavity [10]. However, unlike in strongly-coupled microcavities [5], spontaneous symmetry breaking which is a characteristic feature of the BEC phase transition has not been previously observed in weakly-coupled microcavities.

Here we report on the spontaneous buildup of stochastic polarization vector and long-range coherence in a GaAs quantum-well microcavity, in the strong-coupling regime, where we observe polariton lasing and, surprisingly, also in the weak-coupling photon lasing regime.

Previous studies in this sample have shown both photon lasing under continuous wave excitation [11] and polariton lasing under pulsed excitation [12]. Under high-excitation densities, we have recently observed a dynamical crossover between photon and polariton lasing following a single excitation pulse [13]. This is in agreement with previous observations where increasing carrier density was shown to transfer the system from strong to weak coupling [14, 15].

The total angular momentum \mathbf{J} of a heavy-hole exciton-polariton in a quantum-well microcavity can have two possible projections on the growth axis of the structure, $J_z = +1$ (spin up) or $J_z = -1$ (spin down), corresponding to right and left circularly polarized emitted light, respectively. The order parameter for an exciton-polariton condensate can then be defined by a two-component complex vector $\psi_\sigma(\mathbf{r}, t) = [\psi_{+1}(\mathbf{r}, t), \psi_{-1}(\mathbf{r}, t)]$, where $\psi_{+1}(\mathbf{r}, t)$ and $\psi_{-1}(\mathbf{r}, t)$ are multi-particle wave functions of the spin-up and spin-down components of the condensate. The components of the complex order parameter ψ_σ are related to the measurable condensate pseudo-spin (Stokes vector) \mathbf{S} by $S_x = \text{Re}(\psi_{-1}^* \psi_{+1})$, $S_y = \text{Im}(\psi_{-1}^* \psi_{+1})$, $S_z = (|\psi_{+1}|^2 - |\psi_{-1}|^2)/2$. The components of the Stokes vector are proportional to the linear, diagonal and circular polarization degree of light emitted by the condensate. These polarization degrees define the normalized pseudo-spin vector $\mathbf{s} = 2\mathbf{S}/n$, where n is the occupation number of the condensate. This vector can be quantified experimentally by polarized photoluminescence (PL) measurements [16, 17]. It contains important information on the order parameter of the condensate. The total degree of polarization of the emitted light given by the amplitude of \mathbf{s} changes from zero for a chaotic state to 1 for an ideal condensate. The spontaneous symmetry breaking of the

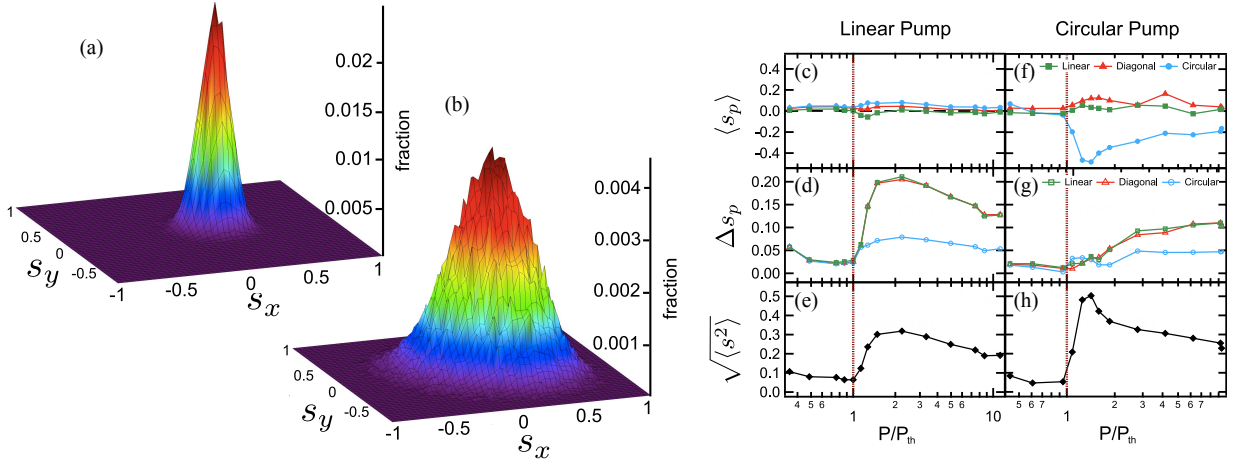


FIG. 1. 2D histogram of linear and diagonal components of the pseudo-spin vector for $P < P_{th}$ (a) and $P = 2.4P_{th}$ (b) on the $x - y$ plane of the Stokes sphere. The mean (c, f), the standard deviation (d, g) and the total degree of polarization (e, h) for linearly (left panel) and circularly (right panel) polarized pump. Above threshold (marked by a red line) we observe the buildup of total degree of polarization while the average polarization remains close to zero for linearly polarized pump.

condensate manifests itself in the spontaneous buildup of polarization of the emitted light [18]. In the absence of pinning, this polarization is randomly chosen by the system and changes stochastically from one experiment to another [19].

The details for the microcavity structure could be found in Ref. [11] and the experimental setup is explained in detail in the Supplemental Material. About 64,000 shots are recorded and analysed for different polarizations and powers of the excitation laser. The components of the normalized pseudo-spin vector \mathbf{s} are measured by $s_{x,y,z} = (I_{0^\circ, 45^\circ, \circ} - I_{90^\circ, -45^\circ, \circ}) / (I_{0^\circ, 45^\circ, \circ} + I_{90^\circ, -45^\circ, \circ})$, where I is the peak intensity of the PL measured to an accuracy of $> 94\%$. Polarization distributions were deconvoluted with the intrinsic noise of the detection system. The PL can be spectrally filtered by means of a grating and an adjustable slit before focusing into the detectors.

Here we measure the polarization of emitted light after each excitation pulse. This measurement is integrated over the lifetime of each individual condensate excited by a laser pulse. On the other hand, we do not average on the ensemble of pulses, but we perform single-shot polarization measurements. Figure 1(a,b) shows the 2D projection of the Stokes parameter histogram on the $x - y$ plane (linear polarization plane) for $\sim 64,000$ shots. In the linear regime and when the pump power is below threshold [Fig. 1(a)] we observe a narrow Gaussian distribution centred to zero, which demonstrates the unpolarized nature of the polariton PL. The width of the Gaussian distribution is limited by the analogue noise and the finite digital sampling rate of the acquisition. Above threshold ($P = 2.4P_{th}$) and still in the strong-coupling regime [Fig. 1(b)] the distribution significantly broadens, with the average polarization again remaining

close to zero. Although the average polarization in the strong-coupling regime is zero we see that each realisation of the condensate is indeed polarized with a random orientation of the Stokes vector.

Fig. 1(c-h) shows the mean degree of polarization, the standard deviation (Δs) and average degree of polarization for linear and circular pump polarization. The increase of standard deviation of polarization in the ensemble of shots is a manifestation of the stochastic buildup of polarization. Contrary to other microcavity samples [20, 21] we do not observe any polarization pinning to the crystallographic axes and below threshold the polarization is unpolarized. The total degree of polarization increases above threshold followed by a sharp drop with increasing pump power.

In the strong-coupling regime the density of electron-hole pairs remains below the Mott transition, where the Coulomb attraction is sufficient to stabilise Wannier-Mott excitons. By increasing the excitation beyond the Mott transition density the excitons ionize and an electron-hole plasma is formed [22, 23]. Energy-resolved Fourier space imaging allows for direct evidence of both the strong and the weak-coupling regime as the corresponding dispersion relations ($E(k)$) are fundamentally different. Above threshold and still in the strong-coupling regime ($P = 1.1P_{th}$) we observe a blue-shifted lower exciton-polariton emission and as we increase the power ($P > 4P_{th}$) we enter the weak-coupling regime and an emission peak near the bare cavity photon energy emerges [13].

Using a grating and a variable mechanical slit we can spectrally filter the photoluminescence emission of polaritons (strong coupling) or bare cavity photon energy states (weak coupling). Fig. 2(a-c) shows the dispersion for the linear, strong-coupling and weak-coupling regime

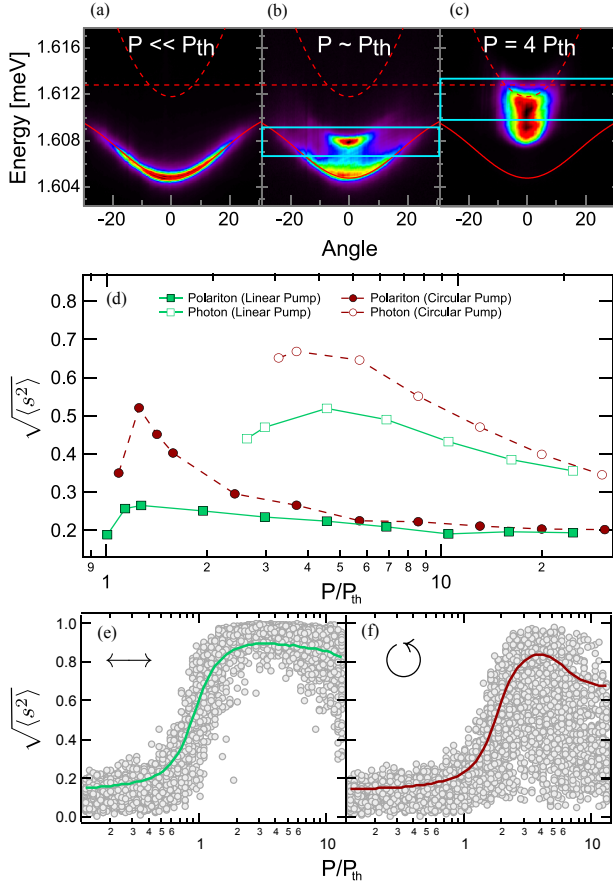


FIG. 2. Dispersion images for (a) below threshold (linear regime), (b) $P = 1.5P_{th}$ (strong-coupling regime) and (c) $P = 4P_{th}$ (weak-coupling regime). The cyan border marks the regions that are filtered for polariton states (b) and bare cavity photon states (c). (d) The total degree of polarization for circularly polarized (dotted lines) and linearly polarized pump (solid lines) for photon (open circles) and polariton energy states (closed circles). (e), (f) Simulation results for the dependence of the total polarization degree on pump intensity for a linearly polarized (e) and circularly polarized (f) pump. The grey circles show the values for each pulse and the solid curves show the root mean square.

respectively. The cyan border displays the energy gap that is filtered for the measurement. Fig. 2(d) shows the total degree of polarization of photon and polariton energy states for linearly and circularly polarized pump. The observed total degree of polarization at bare cavity photon energy is twice higher than that of the polariton states.

A theoretical description of the stochastic polarization buildup in the strong coupling regime can be based on the development of the Langevin equation for exciton-polaritons [19], which replaces the Fokker-Planck equation for distribution functions with a stochastic element. Within this theory, which is described in detail in the Supplementary Information, each pulse in the experiment is modelled separately and receives an influx of polaritons

with random polarization from the hot incoherent excitons excited by the nonresonant pump. Below threshold, the polariton polarization changes rapidly within the duration of each pulse since polaritons excited in the system have uncorrelated stochastic polarization. Equivalently, there is no coherence between polaritons and the total polarization degree (whether averaged over multiple pulses or not) is minimal.

Above threshold, stimulated scattering amplifies the polarization state of polaritons. Polaritons become coherent and a high total polarization degree is expected in each pulse. In the absence of pinning, this polarization is randomly chosen by the system and changes stochastically from one pulse to another. This effect appears both experimentally [Fig. 2(d)] and theoretically [see Fig. 2(f)], however, our theory predicts larger polarization degrees than those observed experimentally. This is to be expected since the theory does not take into account the spatial inhomogeneity of the condensate.

It is important to note that since the average linear polarization degrees observed in our system are minimal [Fig. 1(c)], we expect that only a small polarization splitting is present in the sample. For this reason there is minimal spin relaxation or rotation of the Stokes vector, at moderate densities, after the polarized polariton condensate has formed in each pulse. However, for high polariton densities the anisotropy of polariton-polariton interactions introduces a nonlinear mechanism of Stokes vector precession known as self-induced Larmor precession [24]. This mechanism causes the reduction of the total polarization degree, which is time integrated over the duration of each pulse, for increasing pump intensity in both experiment and theory.

Under circularly polarized pumping the presence of a nonzero circular polarization degree of the polariton condensate demonstrates incomplete spin relaxation of the excited carriers in our experiment [Fig. 1(f)]. Theoretically, this is accounted for by a partial spin relaxation between hot exciton reservoirs. Note that the incomplete spin relaxation does not imply that any phase coherence is preserved from the nonresonant laser.

Our theoretical results demonstrate a lower polarization degree with circularly polarized pumping than with linearly polarized pumping. This is due to increased self-induced Larmor precession when there is a larger imbalance in the spin populations. However, experimentally we rather observe that the polarization degree is lower with linearly polarized pumping. This difference can also be attributed to the spatial degree of freedom, which is not accounted for in our theoretical model. Under linearly polarized pumping, different points in the sample may be polarized differently, in particular since they can have different angles of linear polarization. Under circularly polarized pump, we expect smaller spatial variations in polarization, since the circular polarization is preferred at all points in the sample.

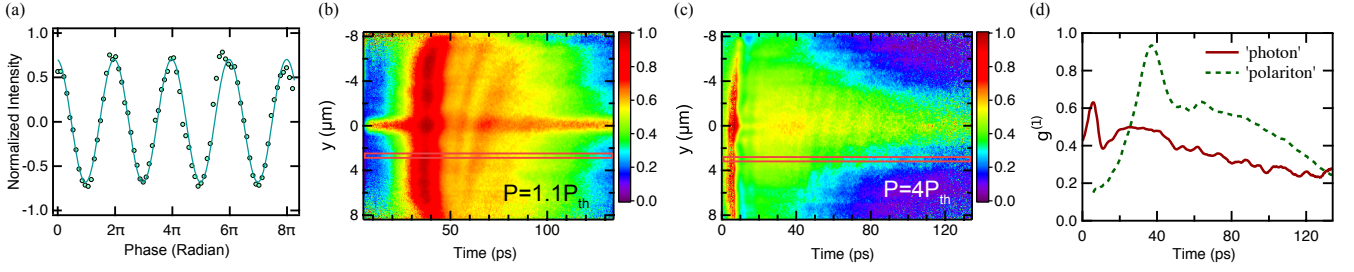


FIG. 3. (a) Normalized intensity on one pixel as a function of phase between the arms of the interferometer. The first-order coherence $g^{(1)}(\mathbf{r}, -\mathbf{r})$ is given by the amplitude. Time resolved first-order spatial coherence, taken across the autocorrelation point at (b) $P = 1.1P_{th}$ and (c) $P = 4P_{th}$. (d) The profile of the first-order coherence as a function of time in polariton and photon laser regimes, at regions y marked in red in (b) and (c).

To reveal the buildup of coherence, the first-order spatial correlation function ($g^{(1)}(\mathbf{r}, -\mathbf{r})$) of the polariton emission is studied using an actively-stabilised Michelson interferometer in a mirror-retro-reflector configuration with close to zero arm length difference (for details see Ref. [2]). To time-resolve the correlation function a diffraction-limited 1-dimensional stripe of the interferograms is sent to a streak camera [25]. By scanning the phase between the mirror and the retro-reflector arm [Fig. 3(a)] $g^{(1)}(\mathbf{r}, -\mathbf{r})$ can be extracted. Time-resolved real-space correlation functions are shown in Figs. 3(b) and Fig. 3(c) for $P = 1.5P_{th}$ and $P = 4P_{th}$ respectively. Fig. 3(b) shows the macroscopic phase coherence for the exciton-polariton condensate. In Fig. 3(c) we observe a high degree of coherence for photon lasing along the whole real space profile. In the transition to polariton lasing the coherence drops significantly and builds up again when the system enters the strong-coupling [Fig. 3(d)], but with a lower degree of coherence due to the lower occupation of the ground state [13].

In Ref. [5] GaN bulk microcavity which is a strongly spatially inhomogeneous system was studied. While this system did show polariton lasing at room temperature and spontaneous vector polarization, it did not show a long-range spatial order, which according to the Penrose-Onsager criterion [1] is a characteristic feature of the phase transition toward Bose-Einstein condensation. The long-range spatial order in polariton condensates was demonstrated by Kasprzak *et al.* [2]. However, they did not observe a stochastic polarization, another key feature of the phase transition which is the spontaneous symmetry breaking. To our knowledge, our present work is the first to show the spontaneous stochastic polarization and long-range spatial coherence in the same structure. We demonstrate that these two crucial features of the phase transition can be observed both in the strong and weak-coupling regime and show theoretical agreement for the exciton-polariton regime.

P.G.L. and A.V.K. acknowledge the FP7 ITN-Spinoptronics, ITN-Clermont 4, Royal Society and EPSRC through contract EP/F026455/1 for funding.

T.C.H.L. acknowledges the support of the European Commission under the Marie Curie Intra-European Fellowship EPOQUES. The authors thank Jacqueline Bloch and Aristide Lemaître for the provision of the sample.

* correspondence address: pavlos.lagoudakis@soton.ac.uk

- [1] O. Penrose and L. Onsager, *Phys. Rev.* **104**, 576 (1956).
- [2] J. Kasprzak, M. Richard, S. Kundermann, A. Baas, P. Jeambrun, J. M. J. Keeling, F. M. Marchetti, M. H. Szymańska, R. André, J. L. Staehli, V. Savona, P. B. Littlewood, B. Deveaud, and L. S. Dang, *Nature* **443**, 409–414 (2006).
- [3] R. Balili, V. Hartwell, D. Snoke, L. Pfeiffer, and K. West, *Science* **316**, 1007 (2007).
- [4] H. Deng, G. Weihs, C. Santori, J. Bloch, and Y. Yamamoto, *Science* **298**, 199 (2002).
- [5] J. J. Baumberg, A. V. Kavokin, S. Christopoulos, A. J. D. Grundy, R. Butté, G. Christmann, D. D. Solnyshkov, G. Malpuech, G. Baldassarri Höger von Högersthal, E. Feltn, J. Carlin, and N. Grandjean, *Phys. Rev. Lett.* **101**, 136409 (2008).
- [6] M. van Exter, A. Jansen Van Doorn, and J. Woerdman, *IEEE J. Sel. Top. Quantum Electron.* **1**, 601 (1995).
- [7] R. Jin, G. Khitrova, D. Boggavarapu, H. M. Gibbs, S. W. Koch, and M. S. Tobin, *J. Nonlinear Opt. Phys. Mater.* **4**, 141 (1995).
- [8] L. V. Butov and A. V. Kavokin, *Nat. Photon.* **6**, 2 (2012).
- [9] B. Deveaud-Plédran, *J. Opt. Soc. Am. B* **29**, A138 (2012).
- [10] J. Klaers, J. Schmitt, F. Vewinger, and M. Weitz, *Nature* **468**, 545–548 (2010).
- [11] D. Bajoni, P. Senellart, A. Lemaître, and J. Bloch, *Phys. Rev. B* **76**, 201305 (2007).
- [12] M. Maragkou, A. J. D. Grundy, T. Ostatnický, and P. G. Lagoudakis, *App. Phys. Lett.* **97**, 111110 (2010).
- [13] E. Kammann, H. Ohadi, M. Maragkou, A. V. Kavokin, and P. G. Lagoudakis, *arXiv:1103.4831* (2011).
- [14] B. Nelsen, R. Balili, D. W. Snoke, L. Pfeiffer, and K. West, *J. App. Phys.* **105**, 122414 (2009).
- [15] J. Tempel, F. Veit, M. Aßmann, L. E. Kreilkamp, A. Rahimi-Iman, A. Löffler, S. Höfling, S. Reitzenstein, L. Worschech, A. Forchel, and M. Bayer, *Phys. Rev. B* **85**, 075318 (2012).

- [16] P. G. Lagoudakis, P. G. Savvidis, J. J. Baumberg, D. M. Whittaker, P. R. Eastham, M. S. Skolnick, and J. S. Roberts, *Phys. Rev. B* **65**, 161310 (2002).
- [17] A. Kavokin, P. G. Lagoudakis, G. Malpuech, and J. J. Baumberg, *Phys. Rev. B* **67**, 195321 (2003).
- [18] F. P. Laussy, I. A. Shelykh, G. Malpuech, and A. Kavokin, *Phys. Rev. B* **73**, 035315 (2006).
- [19] D. Read, T. C. H. Liew, Y. G. Rubo, and A. V. Kavokin, *Phys. Rev. B* **80**, 195309 (2009).
- [20] J. Kasprzak, R. André, L. S. Dang, I. A. Shelykh, A. V. Kavokin, Y. G. Rubo, K. V. Kavokin, and G. Malpuech, *Phys. Rev. B* **75**, 045326 (2007).
- [21] G. Christmann, R. Butté, E. Feltin, J. Carlin, and N. Grandjean, *App. Phys. Lett.* **93**, 051102 (2008).
- [22] L. Kappei, J. Szczytko, F. Morier-Genoud, and B. Deveaud, *Phys. Rev. Lett.* **94**, 147403 (2005).
- [23] M. Stern, V. Garmider, V. Umansky, and I. Bar-Joseph, *Phys. Rev. Lett.* **100**, 256402 (2008).
- [24] I. Shelykh, K. V. Kavokin, A. V. Kavokin, G. Malpuech, P. Bigenwald, H. Deng, G. Weihs, and Y. Yamamoto, *Phys. Rev. B* **70**, 035320 (2004).
- [25] G. Nardin, K. G. Lagoudakis, M. Wouters, M. Richard, A. Baas, R. André, L. S. Dang, B. Pietka, and B. Deveaud-Plédran, *Phys. Rev. Lett.* **103**, 256402 (2009).